

Large-scale mapping of molecular clouds: what can we learn?

F. Massi¹, M. De Luca^{2,3}, D. Elia⁴, T. Giannini², D. Lorenzetti²,
B. Nisini², and F. Strafella⁴

¹ INAF - Osservatorio Astrofisico di Arcetri, Largo Fermi 5, I-50125 Firenze

² INAF - Osservatorio Astronomico di Roma, Via Frascati 33, I-00040 Monteporzio Catone (Roma)

³ Università degli studi di Roma "Tor Vergata", Dip. di Fisica, Via della Ricerca Scientifica 1, I-00133 Roma

⁴ Università di Lecce, Dip. di Fisica, C. P. 193, I-73100 Lecce

Abstract. Molecular line transitions at mm-wavelengths are widely used to study spatial distribution and kinematics of the molecular gas. We present the first results of CO(1–0) line- and 1.2-mm continuum-emission mapping of a molecular cloud in the Vela Molecular Ridge that show the importance of this kind of observations in unveiling the processes underlying diffuse and clustered star formation.

These programs require both high resolution and high sensitivity to diffuse gas (hence, a single-dish telescope is needed). Thus, we also discuss the potentialities offered by the SRT to map relatively large regions of molecular gas, in terms of both available molecular transitions and efficiency.

1. Introduction

One of the main achievements of line observations at 3 mm was the unveiling of the distribution and kinematics of molecular gas within the galactic disk. Lacking suitable transitions of H₂, the lowest rotational ones of CO have proven themselves to be the best tracers. But such large-scale mapping is quite time-consuming and can be carried out only by small telescopes with low resolution. However, the links between gas distribution and star formation regions must be searched for at a much smaller scale, i. e., that of molecular clouds (~ 10 pc). Studying how the structure and kinematics of molecular clouds affect the star formation activity in a region needs not only high sensitivity to large scale diffuse emission, but

also high resolution, to resolve the smallest gas condensations (down to ~ 0.1 pc). In this respect, large single-dish telescopes are needed to meet both prescriptions. Operating large antennas down to mm wavelengths is then appealing.

In this contribution, we will first describe the mapping of a molecular cloud in the southern sky and the main perspectives when complementing it with a study of the star formation activity. This allows one to assess the potential of such kind of observations. Finally, we will evaluate the possible use of the SRT to map relatively nearby molecular clouds, along with its drawbacks.

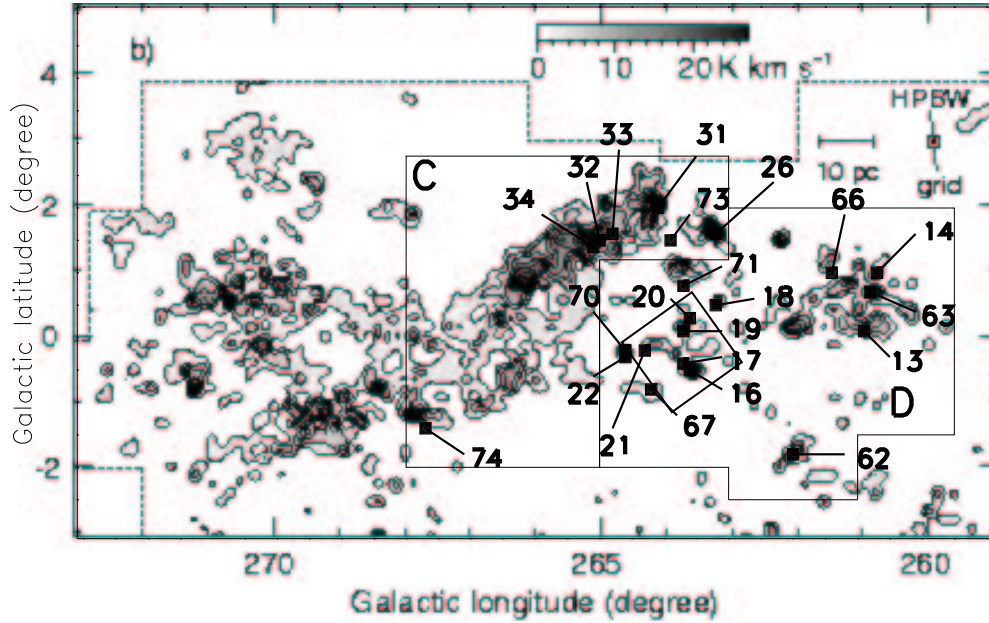


Fig. 1. $^{13}\text{CO}(1-0)$ emission from the Vela Molecular Ridge mapped with the NANTEN telescope (adapted from Yamaguchi et al. 1999 and Massi et al. 2003). Clouds C and D are enclosed with polygons and labeled. The area of the D cloud mapped with the SEST telescope is also enclosed with a square. The IRAS sources studied by Massi et al. (1999, 2000, 2003) are marked with small filled squares and labeled according to the nomenclature adopted by those authors.

2. The importance of CO mapping: the case of the Vela Molecular Ridge

2.1. Outline of the region

The Vela Molecular Ridge (VMR) is a giant molecular cloud complex located outside the solar circle ($257^\circ < l < 274^\circ$) at a kinematical distance of 1–2 kpc, within the galactic disk. It was first mapped in the $\text{CO}(1-0)$ transition by Murphy & May (1991) with the Columbia University millimeter-wave telescope at Cerro Tololo, a 1.2-m antenna. Based on the obtained data (with a resolution of $0.5''$) they could identify four main regions, called A, B, C and D.

The VMR was then mapped with much higher resolution ($2.6''$) by Yamaguchi et al. (1999) using the 4-m millimeter-wave telescope NANTEN at Las Campanas. This led to a significant improvement in our knowledge of gas distribution within the VMR. Figure 1

shows the $^{13}\text{CO}(1-0)$ map obtained by those authors. Fully sampled observations of the same area ($\sim 12^\circ \times 4^\circ$) with large antennas and a single-beam receiver would take prohibitive amounts of time.

Liseau et al. (1992) and Lorenzetti et al. (1993) found a sample of IRAS sources associated with the VMR that may be considered as the analogues of Class I sources (i. e. protostars still in the accretion phase) for intermediate mass ($2 < M < 10 M_\odot$) stars. They also revised the VMR distance, finding that clouds A, C and D lie at 700 ± 200 pc. Hence, these ones are the nearest molecular clouds hosting massive star formation after Orion. Massi et al. (1999, 2000, 2003) studied some of these IRAS sources (all belonging to the C and D clouds) in the Near-Infrared and found that those with $L_{\text{bol}} > 10^3 L_\odot$ are associated with young embedded clusters. Six of these clusters, all belonging to the D cloud, have been further

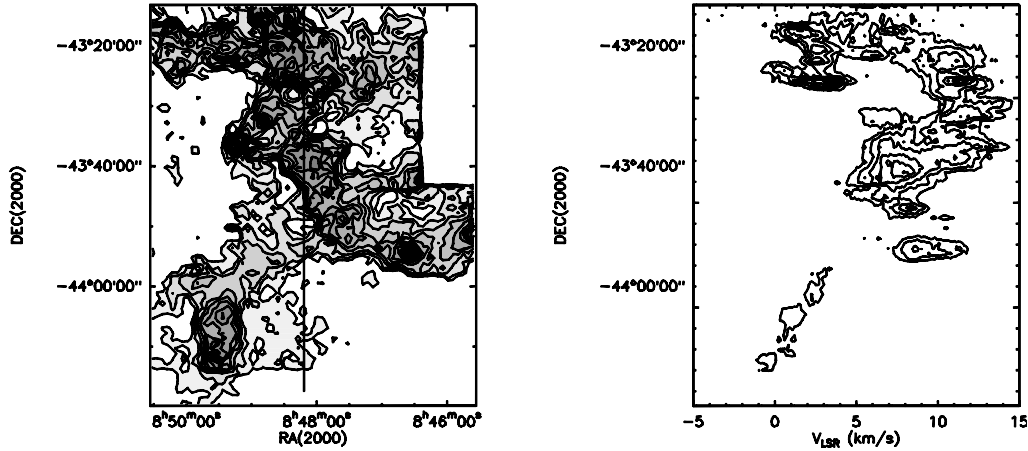


Fig. 2. (a) CO(1–0) map of the cloud D (resolution 43", sampling 50"; SEST data). Contours are from 10 to 190 K km s⁻¹ in steps of 10 K km s⁻¹. (b) Velocity-declination plot along the RA cut indicated by the vertical line in panel a. Contours are 3 to 33 K in steps of 3 K.

studied by Massi et al. (in prep.); they are small (~ 100 members), compact (~ 0.1 pc) stellar groups younger than few 10^6 yrs old with an Initial Mass Function (IMF) compatible with that of field stars.

2.2. Large-scale CO(1–0) map of the D cloud

All previous observations of the VMR allowed us to identify an area of cloud D, roughly 1 square deg, with a high efficiency in forming small star clusters. This is enclosed with a square in Fig. 1 and contains 5 out of the 6 clusters studied by Massi et al. (in prep.). In order to understand the relationship between gas structure (and kinematics) and star cluster formation, in 1999 we mapped this area in CO(1–0) with unprecedented resolution (43") and sampling 50", using the 15-m SEST telescope in La Silla. The spatial resolution at the VMR distance is ~ 0.2 pc, of the order of the size of the hosted clusters and molecular cores. This map is shown in Fig. 2a: the gas exhibits a filamentary structure, with molecular clumps within the filaments. These resemble the edges of shells; that this is the case is confirmed by cuts in Right Ascension like the velocity-declination plot of Fig. 2b. The

velocity-declination plots show shells in a few positions. One is plainly visible in the northern part of Fig. 2b, and another one is sketched in the southern part.

Overlaying the locations of the reddest 2MASS Near-Infrared sources on the CO(1–0) map, it can be seen that the NIR sources tend to be located along the filaments with concentrations towards the emission peaks. These represent not only the already known young stellar clusters, but also as yet unnoticed ones. A possible picture is that expanding bubbles compress the gas triggering the birth of new stars and clusters.

2.3. Tracing the densest gas

Since CO(1–0) has a small critical density and a high optical depth, it is not a good tracer of the densest clumps of gas. Furthermore, CO tends to freeze out in the dust grains at the largest densities. Hence, in 2003 we mapped again the same region of the D cloud, this time in the 1.2-mm continuum using the bolometer array SIMBA on the SEST (see Fig. 3). This allows one to trace the dust thermal emission arising from the dense gas, with a resolution of 25" (~ 0.1 pc).

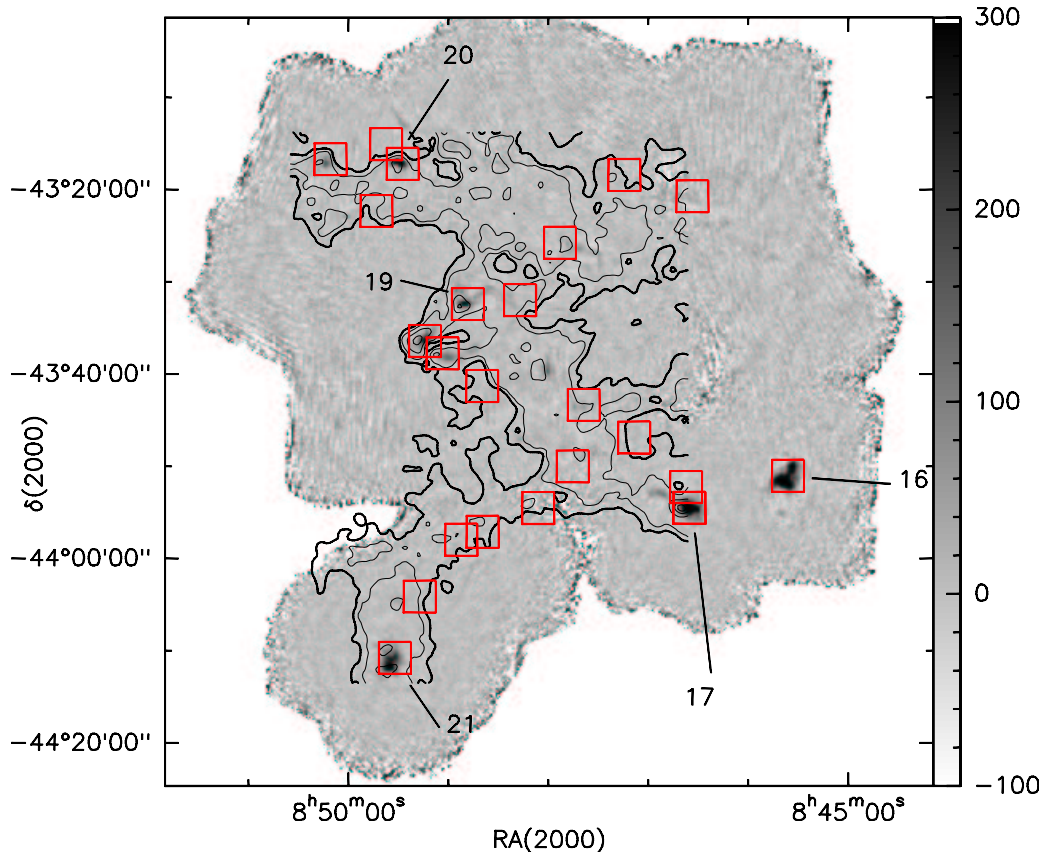


Fig. 3. Map of the 1.2-mm continuum emission from the D cloud (grey scale). Contours sketch the CO(1–0) emission and the reddest IRAS sources’ positions are indicated by squares. Those studied by Massi et al. (1999, 2000) are labeled according to the nomenclature adopted by those authors.

The dust thermal emission reveals small cores within the molecular clumps outlined by CO(1–0). Some of them coincide with red IRAS sources that also follow the gas spatial distribution. By making some assumptions about the dust temperature and opacity, it is straightforward to derive the core masses from the continuum emission. Using an appropriate algorithm (CLUMPFIND, see Williams et al. 1994) we could identify dense (i.e., $10^5 - 10^6 \text{ cm}^{-3}$) cores ranging in mass from few to $\sim 100 M_{\odot}$, with a mass spectrum $N \sim M^{-1.5}$. The spectral index appears as quite standard among similar regions. An insight into the relationships between gas and star formation processes will be obtained by comparing the spec-

tral indices of dust, gas and star cluster mass distribution. Furthermore, the 1.2 mm emission peaks identify targets for future interferometric follow-ups, the only ones able to resolve the smallest cores and derive a mass spectrum to be directly compared with the clusters’ IMF.

A comparison of the masses as derived from CO(1–0) and 1.2-mm continuum emission shows that the clumps identified through CO(1–0) are 2–8 times more massive than the dust cores. This is probably due both to the fact that CO(1–0) traces less dense, more diffuse gas and to the uncertainties in mass determinations. The inferred star formation efficiencies of the clumps are $\sim 0.15 - 0.4$.

Table 1. Line transitions suitable for molecular gas mapping with the SRT. The last column lists typical integration times to reach a $s/n \sim 10$.

Line	Frequency (GHz)	HPBW (arcsec)	Receiver	Int. time
CS(1–0)	48.6	28	6G	13–100 s
CS(2–1)	97.3	14	7G	3.5–21 m
CO(1–0)	115.3	11	8G(?)	18 s

3. Mapping molecular clouds with the SRT

As outlined above, mapping the interstellar medium on the scale of molecular clouds (~ 10 pc) is bound to yield a fundamental insight into the processes starting the fragmentation and collapse of gas and leading to star and cluster formation, when complemented with infrared data. However, the VMR is unusually close-by; massive star forming regions are, on average, much more distant than low-mass star forming regions. Hence, a higher resolution than achieved with telescopes such as the SEST is needed. Assuming that a minimum spatial resolution of 0.1–0.2 pc (i.e., the size of small clusters and molecular cores) is mandatory, the SRT would allow one to carry out the same set of observations as herein described, towards clouds as far as 3 kpc. This would require to map an area $\sim 14' \times 14'$ in a fair amount of time.

The following analysis is based on the parameters given in the “The Sardinia Radio Telescope (SRT). Science and technical requirements” Report (Brand et al. 2005). To assess the mapping capabilities of the SRT at mm-wavelengths, the first step is to identify suitable tracers of relatively diffuse molecular gas, i.e., molecular transitions with low critical densities, high abundances and small level separations, easily detectable using one of the planned receivers. In this respect, the most appropriate transitions are CS(1–0), CS(2–1) and CO(1–0), hoping that observations can be carried out up to 115 GHz. Frequencies and the planned receivers are listed in Table 1. Assuming typical brightness temperatures (1–3 K for CS, 10 K for CO), Table 1 also lists the integration times needed to achieve a signal-

to-noise ratio (s/n) of ~ 10 (using a spectral resolution of 0.1 km s^{-1}). Statistics on the atmospheric transmission at 115 GHz is still unknown for the SRT site. So, we adopted a zenith opacity ~ 0.2 , that is believed appropriate for winter conditions (Olimi, priv. comm.).

Clearly, CO(1–0) and CS(1–0) allow a greater mapping efficiency. Even so, mapping an area of $\sim 15' \times 15'$ in CO(1–0) with sampling ~ 1 beam would take 33.5 hrs (to be multiplied by a factor of 2–3 to account for integration on a reference signal and overhead). Even if this is still an affordable amount of time for a dedicated mm-telescope, it appears to be too long for a telescope operating in such a large range of frequencies and with definite duties (VLBI).

Table 2 compares the performances of the SRT and the IRAM 30-m telescope (Pico Veleta) in observing CO lines. The IRAM 30-m is the largest mm-telescope in Europe and can be operated at the CO(2–1) frequency, yielding the same resolution as the SRT at the CO(1–0) line. Given that such observations can be carried out with HERA, a 3×3 receiver array, it is obvious that the mapping efficiency of the smaller IRAM 30-m telescope is greater than that of the larger SRT 64-m operated at a lower frequency with a single beam receiver.

4. Conclusions

As shown, CO(1–0) at 115.3 GHz is by far the most efficient transition available to map the molecular gas on large scales. Studies of star formation processes can greatly benefit from high resolution and high sensitivity maps of molecular clouds. Hence, it is hopeful that the SRT can possibly be operated up to that frequency. But this requires as soon as possible

Table 2. Comparison of the IRAM 30-m and the SRT. Column 5 lists the integration time on-source to reach a $s/n \sim 10$.

Line	Frequency (GHz)	HPBW (arcsec)	Telescope	Int. time	Notes
CO(1–0)	115.3	11	SRT	18 s	winter
CO(2–1)	230.6	11	IRAM	5 s	good winter
CO(2–1)	230.6	11	IRAM	30 s	average summer

a monitoring effort to characterize the atmospheric transmission at such high frequencies. Also, observational techniques such as on-the-fly mapping have to be developed in order to minimize the overhead.

Whichever the transition that will be available at the SRT to do maps of molecular gas, be it CO(1–0) or CS(1–0), it is clear that the antenna will be scarcely efficient, unless a big receiver array is developed and installed. Only through multi-beam receivers the SRT will be competitive with other available (and older) facilities in operating at high frequencies. On the other hand, only a multi-beam receiver would allow one to optimize the limited timeslot that the SRT schedule can devote to mm-observations and make such observations competitive with respect to the other kinds of possible radio observations within the schedule itself.

Unfortunately, CO is not as good to probe the densest gas structures. The dust thermal emission at mm wavelength appears as one of the most efficient tracers of dense gas, but it requires bolometer arrays. Problems and limitations in developing and using 3-mm bolometer

arrays at the SRT are discussed by Luca Olmi in his contribution to these Proceedings.

References

- Brand, J., Caselli, P., Felli, M., Mack, K.-H., Poppi, S., Possenti, A., Prandoni, I., & Tarchi, A. (Eds.) 2005, ‘The Sardinia Radio Telescope (SRT). Science and technical requirements’, IRA Internal Report 371/05
- Liseau, R., Lorenzetti, D., Nisini, B., Spinoglio, L., & Moneti, A. 1992, *A&A*, 265, 577
- Lorenzetti, D., Spinoglio, L., & Liseau, R. 1993, *A&A*, 275, 489
- Massi, F., Giannini, T., Lorenzetti, D., et al. 1999, *A&AS*, 136, 471
- Massi, F., Lorenzetti, D., Giannini, T., & Vitali, F. 2000, *A&A*, 353, 598
- Massi, F., Lorenzetti, D., & Giannini, T. 2003, *A&A*, 399, 147
- Murphy, D. C., & May, J. 1991, *A&A*, 247, 202
- Williams, J. P., de Geus, E. J., & Blitz L. 1994, *ApJ*, 428, 639
- Yamaguchi, N., Mizuno, N., Saito, H., et al. 1999, *PASJ*, 51, 775